Eur. J. Mech. B/Fluids, **17**, n° 4, 587–594, 1998

A finite-length instability of vortex tubes

D. C. SAMUELS

ABSTRACT. – We show that vortex tubes of finite length have an instability which destroys the vorticity structure quickly. Axial flows develop within the core of the vortex structure, directed inwards from both ends of the vortex tube. The converging axial flows cause the core at the midpoint in length of the vortex tube to expand rapidly, disrupting the vortex structure. Examples of this instability are shown by simulation, and the properties of the instability are derived. In order for the concentrated vorticity structures of turbulence to survive this instability they must be embedded in an external flow which compensates for the self-generated axial flow. This emphasizes the importance of considering the environment of the vortex structures and not just the structures in isolation. © Elsevier, Paris

1. Introduction

The regions of highest vorticity in a turbulent flow take the form of vortex tubes, or "worms". These structures are roughly cylindrical, though some flattening has been observed and the centerlines of these worms are not straight lines (Vincent and Meneguzzu, 1991). For the purposes of this study, we concentrate on the fact that these structures have a finite length. The traditional method of imaging these worms in simulations by plotting all volume elements in the fluid with vorticity above some high threshold actually exaggerates the shortness of these vortex structures, and sometimes previously disconnected structures can be connected into one, longer structure by lowering this threshold (Kerr, 1985). However, these structures do actually have a finite length, which may be defined as where the vorticity level drops to a value near to the r.m.s. level of vorticity in the turbulent flow. These vortex structures are embedded in the turbulent flow, and are both stretched and compressed (Verzicco *et al.*, 1995).

We consider a simple model of a vortex structure that has a cylindrical geometry, but with a finite length, and with a vorticity distribution that satisfies Kelvin's circulation theorem. We model this vortex structure in isolation, so it is not stretched or compressed by any external flow. This allows us to examine the dynamics of the vortex structure itself, and we may later consider how these dynamics could be affected by an external flow. While we are explicitly considering this vortex tube to be a simple model for the vortex worms of turbulence, our results apply to finite-length vortex tubes in general, and may be tested by experiments which can create such individual vortex structures.

2. The model

We choose to model the vortex tube by a vortex filament method (Leonard, 1985). This has the advantage that the initial conditions for a vortex structure with finite length but satisfying the requirement $\vec{\nabla} \cdot \vec{\omega} = 0$ can

Dept. of Mathematics, Univ. of Newcastle, Newcastle-upon-Tyne, NE1 7RU, UK

0997-7546/98/04/© Elsevier, Paris

be easily constructed. The filaments are discretized by placing a number of mesh points along each line. The motion of each mesh point is calculated from the Biot-Savart law

$$\vec{V}_{BS}(\vec{x}_i, t) = \frac{\Gamma_{\text{fil}}}{4\pi} \oint_C \frac{(\vec{\xi} - \vec{x}_i) \otimes d\vec{\xi}}{|\vec{\xi} - \vec{x}_i|^3} \tag{1}$$

where $\vec{x}_i$ is the position of the i'th mesh point, Γ_{fil} is the filament circulation, and the integral is taken over the length of all vortex filaments present in the fluid. To heal the singularity in the Biot-Savart integral, we do not evaluate this integral over the two segments adjacent to the i'th mesh point. This modification to the integral is denoted by the 'C' subscript on the integral (standing for 'cut-off'). To calculate the velocity due to this small, local section of the vortex filament we use the approximation

$$\vec{V}_{\text{local}} = \frac{\Gamma_{\text{fil}}}{8\pi} \log\left(\frac{4l_+ l_-}{a_{\text{eff}}}\right) \vec{S}_i' \otimes \vec{S}_i'' \tag{2}$$

where l_+ and l_- denote the length of the two mesh segments directly adjacant to the mesh point i, a_{eff} is an effective core size of the vortex filament, and $\vec{S}_i'$ and $\vec{S}_i''$ are the local tangent and curvature vectors of the filament. The total velocity of the vortex filament is now just the sum of these two terms $\vec{V}_{\text{total}} = \vec{V}_{\text{total}} + \vec{V}_{BS}$. This choice for the local velocity term gives the correct velocity for a circular vortex ring, and for a straight vortex line, and an approximate velocity for any other configuration. In practice, the local velocity term is always very small.

The results presented here do not depend on the value chosen for the effective core size of the filament, a_{eff}, as long as this parameter is much smaller than the system size. Test simulations with a_{eff} varying by many orders of magnitude (though always remaining small) showed no effect on the instability behaviour reported here. This instability is a property of the large scale flow field, which we are modeling with vortex filaments, and is not an instability of the filaments themselves.

The motion of the vortex filaments is solved by a Runge-Kutta method, to give the development of this flow. No attempt has yet been made to include viscous effects in this simulation, so the motion of the vortices in this calculation is inviscid.

Vortex filament methods have disadvantages as well. A disadvantage which is often overlooked is that one must be careful to separate the dynamics of the *filaments* (which are artificial), from the dynamics of the *vorticity structure*. In particular, the dynamics which one observes must be independent of all the artificial parameters of the vortex filaments introduced to model the flow. These artificial parameters include the number of filaments, the filament core size, and the individual filament circulation. The dynamics of the system must only be affected by the parameters of the macroscopic flow. We have confirmed that this is the case in the simulation results reported here.

We construct our initial vortex structure by placing a number of distorted vortex rings in an azimuthally symmetric distribution, as shown in Figure 1a. The central concentration of vortex filaments represents our vortex tube. To model a tube with finite length, the filaments flare out at the end of the tube, curve around, and re-enter the tube structure at the other end. The distribution of vorticity within the core of the vortex tube can be represented in this model by the spatial distribution of the vortex filaments within the core. The most realistic choice would be to distribute the filaments with a gaussian profile (Jimenez *et al.*, 1993). The next most realistic choice is to use a solid-body rotation model, where the vorticity is uniform within the core radius and zero outside the radius. This is achieved by distributing the vortex filaments on a triangular array with constant spacing between the filaments. The final choice we consider is the hollow-core model where we arrange the filaments only on the surface of the vortex tube structure.

We present results here using the solid-body rotation model and the hollow core model. We see the same dynamics in both models, and on the same time scales. Since the solid-body rotation model is a reasonable approximation to the gaussian distribution, we expect these results to hold for vortex structures with gaussian profiles as well.

3. Evolution of the vortex structure

Once the initial distribution of the vortex filaments is set, we let the filaments move under the Biot-Savart law. An example of the structure's evolution is given in Figure 1. Here we show a hollow core vortex structure modelled by five vortex filaments (*Fig.* 1a). As the structure begins to rotate, a twist develops on the ends of the structure (*Fig.* 1b). This twist is caused by the slow rotation of the ends of the vortex tube, compared with the rotation of the middle of the tube. The regions of twist move inwards along the core of the vortex tube until they meet (*Fig.* 1c). The collision of these twisted regions results in the rapid expansion of the vortex tube core in a small section at the middle of the tube. This localized expansion continues, and the core of the entire vortex tube also continues to expand, disrupting the original vortex structure (*Fig.* 1d).

We can make a quantitative measurement of the disruption of this structure by measuring the vortex tube radius in the centerplane of the structure ($z = 0$, where the structure extends from $-L_{\text{struct}}/2$ to $L_{\text{struct}}/2$). We define this radius as the largest radial position of a vortex filament with negative orientation (the orientation of the central vortex cylinder) passing through the $z = 0$ plane. This measurement is plotted in Figure 2. We show here measurements from four simulations, each modelling the same macroscopic vortex structure, with different arrangements of vortex filaments. Two simulations used a hollow core arrangement, with 3 and 5 filaments respectively. The other two simulations used a solid-body rotation arrangement with 7 and 19 filaments. The parameters of the macroscopic vortex tube were kept constant over these four simulations. A gaussian distribution has not been used yet due to the difficulty of measuring a radius in that model (compared to the simple definition for these two models). All four simulations show the same instability behavior, on identical time scales. This shows that the instability behavior is a behavior of the vortex tube, and not of the model filaments. Surprinsingly, there was little difference between the two core models. The only observable difference is that the hollow core model simulations showed some significant oscillations in radius immediately prior to the rapid radius growth, while the solid-body rotation models had a very slow, but fairly steady, growth in radius before the very rapid radial expansion began. These differences are not yet understood. For the remainder of this paper we will concentrate on the time required for the instability to develop, which is the same for these two core models, and which presumably would be the same for a realistic gaussian distribution as well.

Figure 2 presents data for the radius containing a given circulation, which is a natural measurement for a vortex filament calculation. In continuum calculations it is more natural to speak in terms of vorticity. We can roughly convert our measurement to these terms by making the definition

$$\omega_{\text{struct}} = \Gamma_{\text{struct}}/\pi r_{\text{core}}^2 \tag{3}$$

where ω_{struct} is the vorticity of the vortex tube, in the midplane and averaged over the vortex tube core, and r_{core} is the measured core radius of the tube. This measurement is plotted in Figure 3. The higher power of the radius in this plot accentuates the effects of the instability. This instability should appear as a very rapid drop, locally, of the vorticity at a position along the vortex tube.

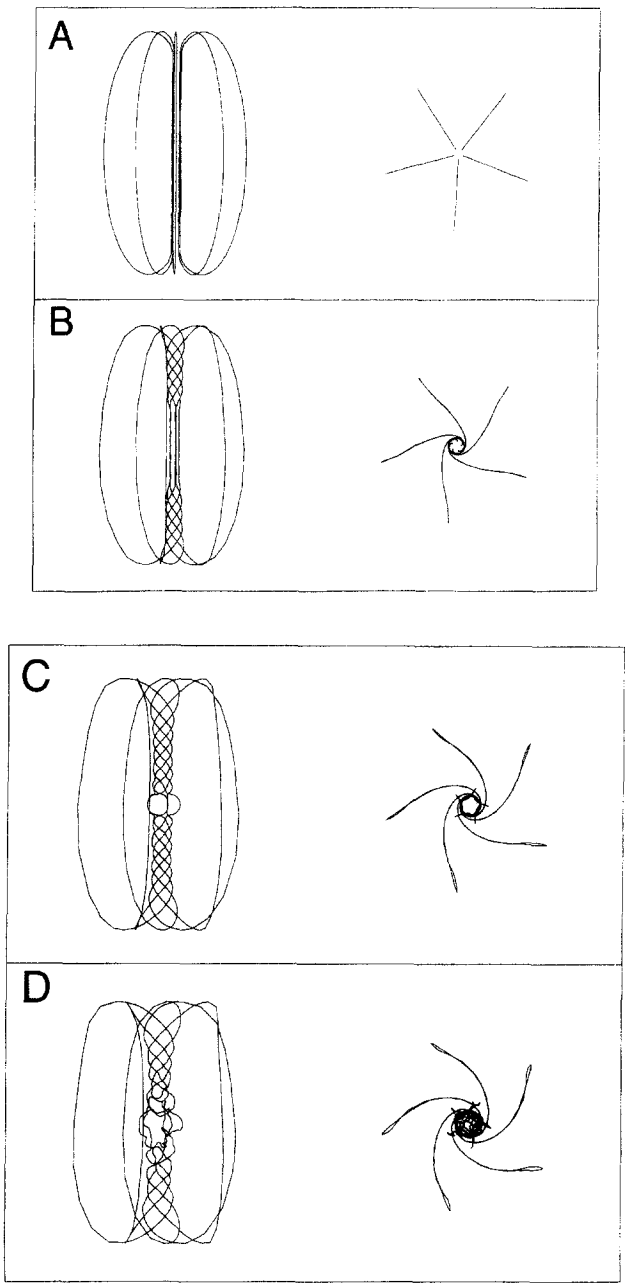

Fig. 1. – Motion of the vortex filaments. Front and top views. (A) $t = 0$, (B) $t = 2.8$ rotations, (C) $t = 5.8$ rotations, (D) $t = 8.7$ rotations.

4. Axial flow

To understand the instability, we must consider the axial flow V_z within the core of the vortex tube. This brings us to another disadvantage of vortex filament calculations: the filaments cause large, and artificial, velocity spikes near each filament. In practical terms, this means that accurate velocity measurements are limited to regions that do not contain the filaments. This presents a problem for measuring the axial velocity within the center of the vortex tube. We overcome this problem by making axial flow measurements only on the hollow-core

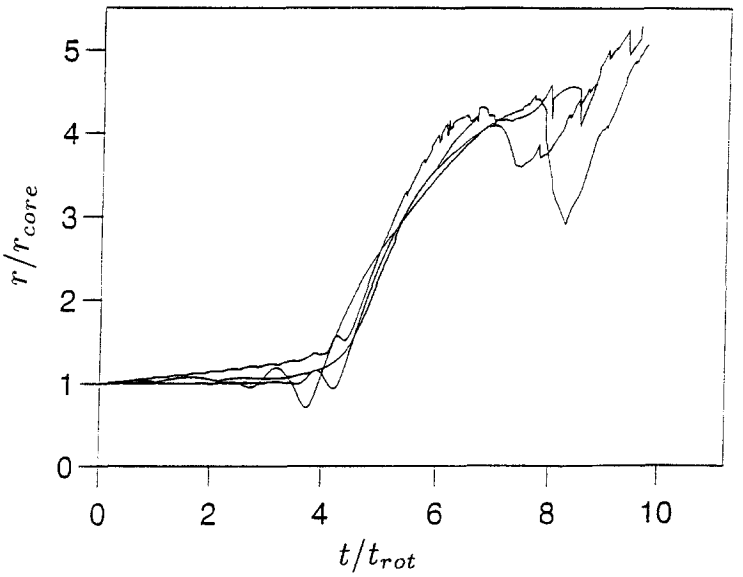

Fig. 2. – Measured radius of the vortex tube in the midplane. The data are from four simulations; two hollow-core models with 3 and 5 filaments and two solid-body rotation models with 7 and 19 filaments.

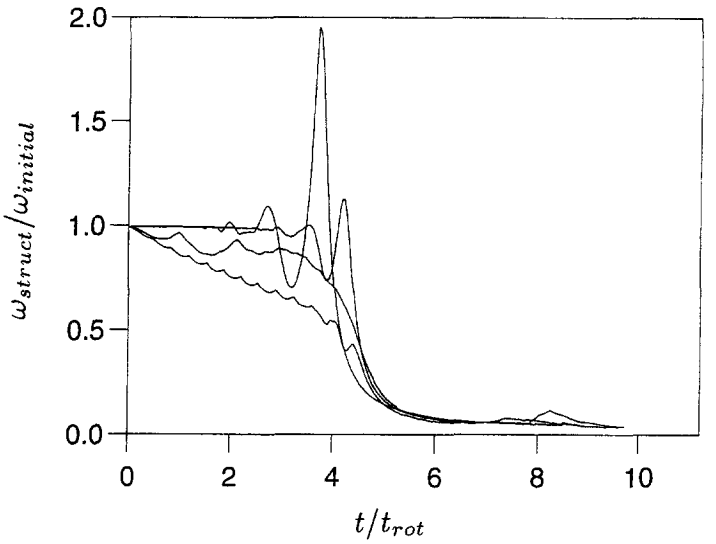

Fig. 3. – Local vorticity in the midplane averaged over the width of the vortex structure core.

model simulations, since these models do not contain vortex filaments very near the centerline, where we wish to measure the velocity. This is our only reason for considering a hollow-core model.

The initial vortex structure has no axial flow. As the vortex structure evolves, and the regions of twist form, corresponding regions of axial flow develop (*Fig.* 4). These axial flows are directed inward from each end of the tube. When the regions of twist collide, so do the regions of axial flow. This results in a very sharp gradient $\partial V_z/\partial z$ over a small length of the tube, here only a few core radii in length. By incompressibility,

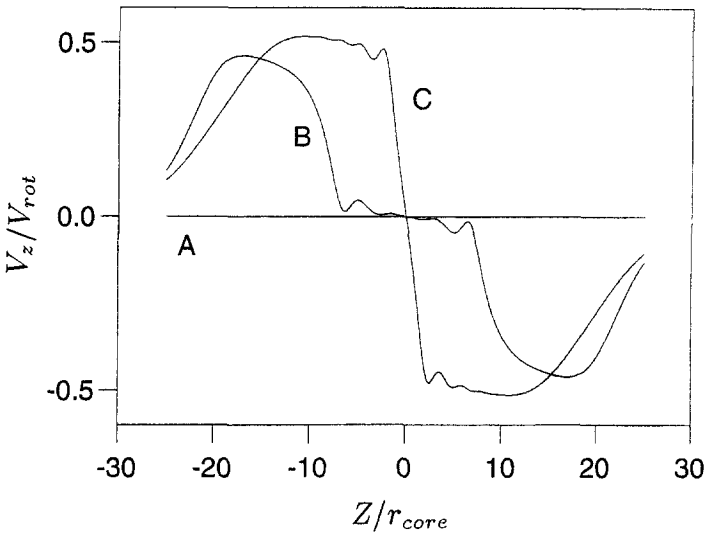

Fig. 4. – Axial flow V_z measured within the vortex tube core. Letters A, B, and C refer to the time of Figure 1.

and assuming that the instability is axisymmetric, this causes a large and localized radial flow outward, which is seen in Figure 1c as a rapid core expansion.

The inner edges of the regions of axial flow are fairly sharp, and they move inward with a well defined velocity $V_{\text{front}} = \alpha V_{\text{rot}}$, where $V_{\text{rot}} = \Gamma_{\text{struct}}/2\pi r_{\text{core}}$ is the peak rotational velocity of an infinitely long vortex tube with the circulation and core size of the tube we are modelling. From a series of simulations with varying parameter values we find that the value of the constant of proportionality is $\alpha = 0.83 \pm 0.03$. This is in very good agreement with the maximum speed of the axisymmetric bulging mode on a vortex tube (Saffman, 1992). Together with the observation that the regions of twist do also involve an axisymmetric increase in the radius (*Fig.* 1b), we can infer that the motion of the regions of axial flow (and hence the time of the instability) is limited by the speed of bulging modes on the vortex tube.

It is surprising that we get the result that $V_{\text{front}} = (0.83 \pm 0.03)V_{\text{rot}}$ for all of our simulations, both the solid core and hollow core vortex tubes. This is the speed of bulging modes on a vortex tube with a solid-body rotation core. We do not yet have an explanation for why we see the same front velocity in both core models. Perhaps this is because our two examples of 'hollow-core' models are done at quite a low resolution, with only 3 and 5 filaments in each model. At this low a resolution the difference between the 'solid-body rotation' and the 'hollow' core is actually negligable. The two 'hollow core' models should more properly be considered to be just low resolution models of the vortex tube, too low to distinguish a core structure. The solid body core rotation models contained a higher number of filaments, and of the two core models the solid-body rotation model is the most realistic.

The instability described here is related to axisymmetric vortex breakdown (Leibovich, 1978). In both cases, a stagnation point forms in the vortex core (*Fig.* 4), leading to the local expansion of the core. A difference between this instability and the "traditional" vortex breakdown is that in the traditional case an initial, uniform axial flow is assumed, and a region of reversed flow is generated to form the stagnation point, while in this instability no axial flows are initially present. Both positive and negative axial flows are self-generated by the vortex. These regions of axial flows move towards each other, form the stagnation point (and hence a high axial velocity gradient), and cause the core expansion.

5. Time scales

With a well defined velocity, we can define an instability time simply as the time required for the axial flow regions to move over half the length of the vortex tube (and then collide). This time is

$$t_{\text{inst}} = (L_{\text{struct}}/2)/V_{\text{front}} = \pi L_{\text{struct}} r_{\text{core}}/\alpha\Gamma_{\text{struct}} \tag{4}$$

The most natural time scale to compare this instability time to is the rotational period of the structure (again, assumed infinitely long). This ratio is

$$t_{\text{inst}}/t_{\text{rot}} = (1/4\pi\alpha)(L_{\text{struct}}/r_{\text{core}}) \tag{5}$$

From this we see that longer vortex tubes will survive for more rotations before this instability begins to disrupt the core.

Since we are primarily concerned with this instability in the context of the concentrated vortex tubes of turbulent flows, we should consider the instability time scaled with turbulence time and length scales that are relevant to the turbulence vortex worms. With that in mind, we scale the time by the large eddy turnover time t_0, the length L_{struct} by the integral length scale L, the tube radius by the Kolmogorov length scale η, and the tube circulation by the kinematic viscosity ν (Jimenez *et al.*, 1993). The result is

$$\frac{t_{\text{inst}}}{t_0} = \frac{\pi}{\alpha}\left(\frac{L_{\text{struct}}}{L}\right)\left(\frac{r_{\text{core}}}{\eta}\right)\left(\frac{\Gamma_{\text{struct}}}{\nu}\right)^{-1}\left(\frac{\eta}{\lambda}\right)\text{Re}_\lambda \tag{6}$$

where λ is the Taylor microscale and Re_λ is the Taylor microscale Reynolds number.

Using the turbulence relationship $\eta/\lambda \sim \text{Re}_\lambda^{-1/2}$ and the observation from simulations that $\Gamma_{\text{struct}}/\nu \sim \text{Re}_\lambda^{1/2}$ (Jimenez *et al.*, 1993) we arrive at the unexpected conclusion that the ratio t_{inst}/t_0 is independent of Reynolds number, assuming that the ratios L_{struct}/L and r_{core}/η are also independent of Reynolds number, as seems to be the case in simulations (Jimenez *et al.*, 1993). This result must be considered sceptically, however, since we have not yet taken into account any effects from vortex stretching or compression, which are strongly present in turbulence vortex structures.

6. Conclusions

We have described a particular instability which disrupts vortex tubes with finite length. Has this been observed? And do our descriptions of the axial flows and the instability time scale agree with measurements? In recent numerical simulations of turbulence generated by gravity waves, Arendt *et al.* (1997 and 1998) observed the formation and subsequent destruction of concentrated vortex tubes. In the period just prior to the destruction of the vortex tubes, strong axial flows developed within the tube, similar to the pattern shown in Figure 4. Vortex lines calculated from the flow at this time showed twisted vortex lines corresponding closely to those formed in our simulations (*Fig.* 1b). This is a good indication that, in at least some turbulent flows, this instability acts to destroy vortex structures. Melander and Hussain (1994) have observed in simulations the transient appearance and disappearance of low enstrophy pockets with a tubular vortex structure. This is quite likely to be an observation of the same instability reported here.

In experiments which can image the cores of the vortex tubes (generally with gas bubbles in liquid flows) the instability should be observable as a local expansion of the core size at a position near the middle of the

vortex tube. Behavior quite similar to this description has been observed in the experiments of Cadot *et al.* (1995). It would be interesting if these measurements could be extended to include axial flow measurements as well as core imaging.

Perhaps the most fruitful approach to studying this instability in experiment would be to create individual vortex tubes in a controlled manner. The experiments of Pinton *et al.* (1997) do just this, by forming a single vortex extending between two spinning disks. These vortices are observed to be unstable, and the measured time for the instability to occur does agree well with that predicted in Eq. (5) (Pinton, personal communication).

In order to interpret this instability in terms of the vortex structures present in turbulence, we still must understand how this instability is changed by axial stretching and compression of the vortex structure. This remains to be done. As a naive first approximation, we would predict that the stretching would have to be strong enough to prevent the self-generated axial flows from reaching the center of the vortex tube and then colliding. This would require a stretching velocity greater than $V_{\text{front}} = 0.83 V_{\text{rot}}$ near the ends of the tube. Of course, this is only a first approximation, and non-linear effects, such as the compression of the vortex core during axial stretching may change this limit. And finally, we must remember the turbulence simulations of Arendt *et al.* (1997 and 1998) which do see this instability destroying vorticity structures in a turbulent flow. The instability may have a role to play in determining some statistics of the turbulent vortex structures simply by destroying those structures which are short (see Eq. (5)) or which are insufficiently stretched.

REFERENCES

ARENDT S., FRITTS D. C., ANDREASSEN O., 1998, "Twist waves and the transition to turbulence", *Eur. J. Mech. B*, submitted.

ARENDT S., FRITTS D., ANDREASSEN O., 1997, "The initial value problem for Kelvin vortex waves", *J. Fluid Mech.*, **344**, 181-212.

CADOT O., DOUADY S., COUDER Y., 1995, "Characterization of the low-pressure filaments in a three-dimensional turbulent shear flow", *Phys. Fluids*, **7**, 630-646.

JIMENEZ J., WRAY A. A., SAFFMAN P. G., ROGALLO R. S., 1994, "The structure of intense vorticity in isotropic turbulence", *J. Fluid Mech.*, **255**, 65-90.

KERR R. M., 1985, "Higher order derivative correlations and alignment of small scale structures in isotropic numerical turbulence", *J. Fluid Mech.*, **153**, 31-58.

LEIBOVICH S., 1978, "The structure of vortex breakdown", *Ann. Rev. Fluid Mech.*, **10**, 221-246.

LEONARD A., 1985, "Computing three-dimensional incompressible flows with vortex elements", *Ann. Rev. Fluid Mech.*, **17**, 523-559.

MELANDER M. V., HUSSAIN F., 194, "Core dynamics on a vortex column", *Fluid Dynamics Research*, **13**, 1-37.

PINTON J.-F., CHILLA F., MORDANT N., 1997, "Intermittency in the closed flow between coaxial corotating disks", pre-print.

SAFFMAN P. G., 1992, *Vortex dynamics* (Cambridge, Cambridge).

VERZICCO R., JIMENEZ J., ORLANDI P., 1995, "On steady columnar vortices under local compression", *J. Fluid Mech.*, **299**, 367-388.

VINCENT A., MENEGUZZI M., 1991, "The spatial structure and statistical properties of homogeneous turbulence", *J. Fluid Mech.*, **225**, 1-20.

(Received 31 July 1997,
revised 13 February 1998,
accepted 03 March 1998)